

Collectivity of J/ψ Mesons in Heavy-Ion Collisions

Min He¹, Biaogang Wu², and Ralf Rapp²

¹*Department of Applied Physics, Nanjing University of Science and Technology, Nanjing 210094, China* and

²*Cyclotron Institute and Department of Physics and Astronomy,
Texas A&M University, College Station, Texas 77843-3366, U.S.A.*

(Dated: November 29, 2021)

The production of J/ψ mesons in heavy-ion collisions at the Large Hadron Collider is believed to be dominated by the recombination of charm and anti-charm quarks in a hot QCD medium. However, measurements of the elliptic flow (v_2) of J/ψ mesons in these reactions are not well described by existing calculations of J/ψ recombination for transverse momenta $p_T \gtrsim 4$ GeV. Here, we revisit these calculations in two main aspects. By employing the resonance recombination model, we implement distribution functions of charm quarks transported through the quark-gluon plasma using state-of-the-art Langevin simulations, and we account for the space-momentum correlations of the diffusing charm and anti-charm quarks in the hydrodynamically expanding fireball. These improvements extend the relevance of the recombination processes to substantially larger momenta than before. In addition, we revisit the suppression of the primordially produced J/ψ mesons by propagating them through the same hydrodynamic medium, leading to a marked increase of the v_2 of this component over previous estimates. Combining these developments into a calculation of the p_T -dependent nuclear modification factor and v_2 of inclusive J/ψ production in semi-central Pb-Pb(5.02 TeV) collisions, we find a good description of the experimental results by the ALICE collaboration. Our results thus resolve the above-mentioned v_2 puzzle and imply the relevance of recombination processes for p_T 's of up to ~ 8 GeV.

PACS numbers: 25.75.-q 25.75.Dw 25.75.Nq

Introduction.— Heavy quarkonia have long been proposed as a probe of deconfinement in the hot and dense QCD medium formed in high-energy heavy-ion collisions [1–5]. Based on the understanding of their vacuum spectroscopy using the well-established Cornell potential, the main binding of charmonium states is indeed generated by the linear potential term commonly associated with the confining force. Lattice-QCD (lQCD) computations of the free energy of a static quark-antiquark pair suggest that the confining force may survive to temperatures significantly higher than the pseudo-critical temperature, T_{pc} , of the chiral phase transition. The suppression of initially produced charmonia in the hot medium will be followed by a subsequent “regeneration” once bound-state formation is supported again, where inelastic reaction rates will drive the charmonium abundances toward their equilibrium values. At which temperatures the different bound states (re-)emerge, and whether and how they reach equilibrium, are intensely debated questions at present. The answers will depend on the microscopic interplay of the in-medium potential screening and the inelastic reaction rates.

High-energy heavy-ion collisions at the Super Proton Synchrotron (SPS), Relativistic Heavy-Ion Collider (RHIC) and the Large Hadron Collider (LHC) have provided a wealth of data on both charmonia and bottomonia. The former are rather strongly suppressed at SPS and RHIC energies, relative to the baseline from proton-proton (pp) collisions, but have shown a remark-

able increase in their nuclear modification factor in semi-central Pb-Pb collisions at the LHC [6–9]. This rise has been predicted by both the statistical hadronization model [10] and transport approaches [11–13], albeit the predictions differ appreciably in detail. The presence of regeneration processes has been further corroborated by the experimental findings that the increased yield is largely concentrated at low transverse momenta, $p_T \lesssim 3$ GeV, and by an appreciable elliptic flow (v_2) [14] which has been associated with the large elliptic flow of the recombining charm quarks as found in D -meson observables. However, predictions based on transport model calculations [15, 16], which give a fair description of the centrality and p_T -dependence of J/ψ production in Pb-Pb collisions at the LHC, fall significantly short of the experimentally measured v_2 of J/ψ 's with transverse momenta $p_T \gtrsim 4$ GeV. These calculations approximated the p_T dependence of the regenerated J/ψ 's by a thermal blastwave ansatz (which implies thermalized anti-/charm quark spectra), and also the elliptic flow of the primordial component was schematically (and conservatively) estimated to level off at a value of ~ 2 –3% which under-predicts the data at high p_T . In the present paper we will remedy these approximations by evaluating the recombination processes with state-of-the-art charm-quark distributions following from relativistic Langevin simulations that give a fair description of open heavy-flavor observables at the LHC [17]. In this way we establish, for the first time, a quantitative connection between the trans-

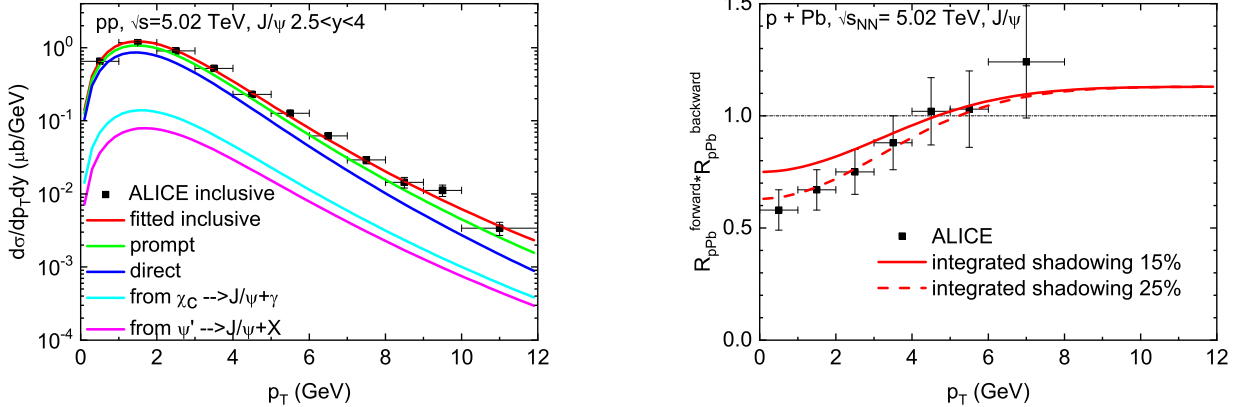


FIG. 1: Left panel: Inclusive (red line) and prompt (green line: total, blue line: direct, cyan and pink line: χ_c and ψ' feeddown) J/ψ spectra in 5.02 TeV pp collisions, compared to ALICE data [6]. Right panel: shadowing function (upper(lower) line for 15(25)% total shadowing) compared to ALICE data [23] for the forward times backward R_{pA} in $p\text{-Pb}$ collisions.

port of open and hidden charm sectors in high-energy nuclear collisions. We will also revisit the computation of the v_2 of the suppressed primordial J/ψ component within the same hydrodynamic model as used for the charm-quark transport.

Primordial J/ψ 's and their Suppression .– A common observable to characterize the hard production of particles in high-energy heavy-ion (AA) collisions, relative to that in proton-proton (pp) collisions at the same energy, is the nuclear modification factor defined as

$$R_{\text{AA}}^{\text{incl}}(p_T) = \frac{dN_{\text{incl}}^{\text{AA}}/dp_T dy}{\langle T_{\text{AA}} \rangle d\sigma_{\text{incl}}^{pp}/dp_T dy}, \quad (1)$$

where the numerator denotes the particle spectrum in an AA collision for a given centrality selection, and $\langle T_{\text{AA}} \rangle$ is the pertinent nuclear thickness function [18]. To construct the inclusive J/ψ cross section in pp collisions, $d\sigma_{\text{incl}}^{pp}/dp_T dy$, we fit pertinent ALICE data [6] at 5.02 TeV using a power-law fit, $d\sigma/dp_T dy = C p_T / (1 + (p_T/p_0)^2)^m$ with $p_0 = 3.8 \text{ GeV}$ and $m = 3.73$, cf. Fig. 1. Upon subtracting the measured p_T -dependent fraction of non-prompt J/ψ which arise from b -hadron feeddown [19, 20], the prompt J/ψ differential cross section is obtained, which is further decomposed into direct J/ψ 's and feeddown contributions from χ_c and ψ' decays [21, 22].

Next, we implement nuclear shadowing. Since we are mainly interested in ALICE dimuon data (where the most precise J/ψ data in AA collisions are available), taken for rapidities $2.5 < |y| < 4$, we fit the measured product of the forward and backward nuclear modification factor of J/ψ production in $p\text{-Pb}$ collisions, R_{pA} , cf. Fig. 1, allowing for a variation of an integrated shadowing suppression of 15%-25% for mid-central collisions.

The suppression of primordial charmonia, $\Psi = J/\psi$, χ_c and ψ' , in Pb-Pb collisions starts from the “shadowed”

p_T -differential cross section and the spatial binary collision density function, $n_{\text{BC}}(x, y)$, for their initial conditions. Their straight-line motion through the hydrodynamic medium used in Ref. [24] (which is tuned to light-hadron data at each centrality) is simulated on an event-by-event basis in a smooth hydrodynamic background, with quasifree dissociation rates and formation time effects from the transport approach of Ref. [16], until the Ψ enters a cell at the kinetic freezeout temperature (e.g., $T_{\text{kin}} \simeq 110 \text{ MeV}$ for 20-40% central Pb-Pb). Following previous approaches, elastic rescattering is neglected, as it is parametrically suppressed. Since direct- J/ψ production dominates the p_T -differential cross section of prompt J/ψ 's in pp collisions, and since the excited states χ_c and ψ' are substantially stronger suppressed, the left-over prompt contribution shown in Fig. 2 is essentially given by the surviving direct J/ψ 's. The magnitude and shape of the p_T spectra are in fair agreement with the fireball calculations of Ref. [16], but the elliptic flow, levelling off at $\sim 5\%$ toward large p_T in semicentral collisions (see right panel of Fig. 2), is significantly larger than the earlier schematic estimates [15, 25–27], amounting to up to 2-3%. In addition to the usual path-length dependence for the suppression along the short vs. long axis of the almond-shaped nuclear overlap zone, an important effect arising from the hydrodynamic simulation is that the density profile is more compressed along the short axis and thus drops faster toward the boundary. As a consequence, the outward Ψ propagation along the short axis on average encounters less dense regions than along the long axis, implying on average smaller dissociation rates.

J/ψ Regeneration.– To compute the p_T -dependence of the regeneration component, we employ the resonance recombination model (RRM) [28], which is a 4-momentum conserving hadronization model based on the Boltzmann

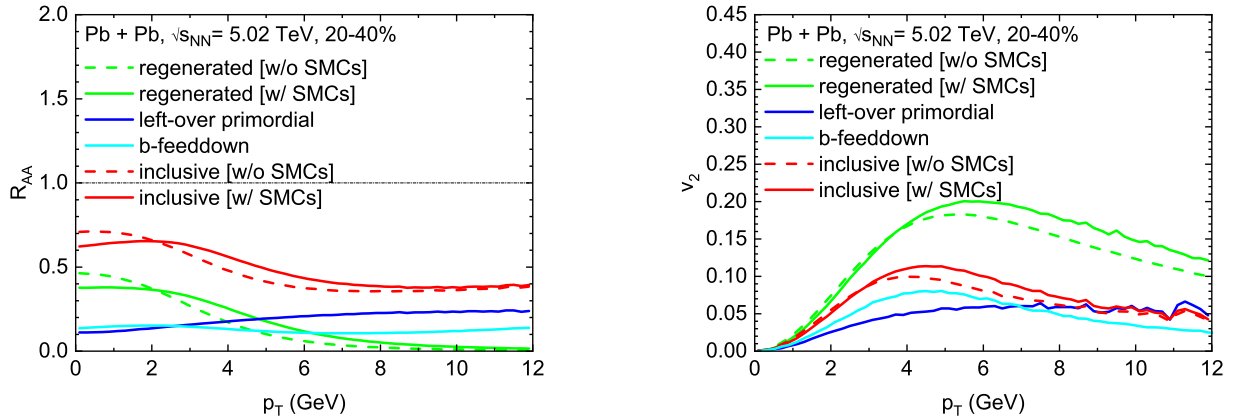


FIG. 2: J/ψ R_{AA} (left) and v_2 (right) in 20-40% 5.02 TeV PbPb collisions with 15% integrated shadowing for inclusive production (red lines), regeneration (green lines) and primordial components (blue lines), and bottom feeddown (cyan line). For the inclusive and regeneration contributions, the solid (dashed) lines are calculated with(out) SMCs.

equation that recovers the correct equilibrium distribution of the produced hadron if the underlying quark distributions are in equilibrium (which also holds for the situation of moving media [29], including the v_2). In its current implementation, the RRM does not predict the absolute norm of the produced hadrons. Therefore, we take recourse to our previous transport calculations for 3-momentum integrated Ψ yields. These are obtained from solving the kinetic-rate equation,

$$\frac{dN_\Psi^{\text{reg}}(\tau(T))}{d\tau} = -\Gamma_\Psi(T)[N_\Psi^{\text{reg}}(\tau(T)) - N_\Psi^{\text{eq}}(T)] , \quad (2)$$

in an expanding fireball medium, where the equilibrium limit, $N_\Psi^{\text{eq}}(T)$, follows from relative chemical equilibrium of the time-evolving charm content of the system (c -quarks in the QGP and charm hadrons in the hadronic phase, with total charm-quark number conserved). The inelastic reaction rates, Γ_Ψ , are the same as used for the suppression calculation discussed above [16]. Based on detailed balance, we can then utilize the regeneration yield of the rate equation to normalize the RRM yields.

Within the RRM, the p_T -spectrum of the regenerated Ψ states is given by

$$f_\Psi(\vec{x}, \vec{p}) = C_\Psi \frac{E_\Psi(\vec{p})}{m_\Psi \Gamma_\Psi} \int \frac{d^3 \vec{p}_1 d^3 \vec{p}_2}{(2\pi)^3} f_c(\vec{x}, \vec{p}_1) f_{\bar{c}}(\vec{x}, \vec{p}_2) \times \sigma_\Psi(s) v_{\text{rel}}(\vec{p}_1, \vec{p}_2) \delta^3(\vec{p} - \vec{p}_1 - \vec{p}_2) , \quad (3)$$

where $f_{\bar{c},c}$ are the transported phase space distributions of anti-/charm quarks, and v_{rel} is their relative velocity. In the current $2 \rightarrow 1$ formulation, hadronization is realized via a resonance cross section, $\sigma_\Psi(s)$, for $c + \bar{c} \rightarrow \Psi$, taken of Breit-Wigner form with the vacuum Ψ pole masses and widths $\Gamma_\Psi \simeq 100$ MeV, while the C_Ψ ensure the normalization following from the rate equation. The anti-/charm-quark phase space distributions are taken from recent Langevin simulations of

charm-quark diffusion in the QGP that result in a successful phenomenology of open HF observables at the LHC [17, 24]. In particular, the RRM enables to incorporate space-momentum correlations (SMCs) [24], here for the charm and anticharm quarks, on an event-by-event basis from the Langevin simulations. In the rate equation approach, the production of different charmonium states occurs over a finite temperature range [12]. Following the procedure adopted before where the J/ψ blastwave spectra were evaluated at an *average* temperature of $T=180$ MeV [16], we here evaluate the RRM on a hydrodynamic hypersurface at a constant longitudinal proper time, $\tau_f \simeq 5.2$ fm/ c for semi-central Pb-Pb(5 TeV) collisions, yielding a range of average temperatures of $T=170$ -190 MeV, cf. the red histogram in Fig. 3. Since the temperature window for regeneration is related to the dissociation temperature of the various Ψ states, we also consider a 20% earlier freezeout time, $\tau_f \simeq 4.2$ fm/ c , resulting in a significantly higher range of average regeneration temperatures, cf. the green histogram in Fig. 3.

In Fig. 2 left we display the R_{AA} of regenerated prompt J/ψ 's in 20-40% Pb-Pb(5 TeV) collisions. Compared to earlier thermal blastwave approximations [15, 16], the RRM spectra with transported charm-quark distributions are appreciably larger for $p_T \gtrsim 3$ GeV. The inclusion of SMCs is also quite noticeable, enhancing the result without SMCs for $p_T \gtrsim 3$ GeV, *e.g.*, by a factor of ~ 2 at $p_T \simeq 6$ GeV, where the recombination contribution is still rather significant relative to the primordial one. The resulting v_2 for the RRM component, shown in Fig. 2 right, is much larger than for the primordial one, reaching up to $\sim 20\%$; also here the SMCs lead to a moderate increase, by ca. 10-20% for $p_T > 4$ GeV. However, for the inclusive v_2 , the extended reach of the regeneration yield due to the SMCs is more relevant, causing an

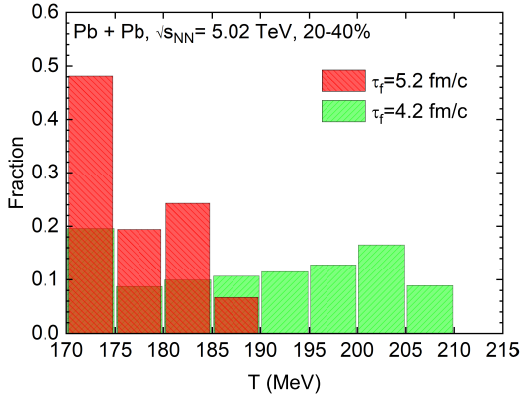


FIG. 3: Temperature distribution of regenerated J/ψ 's as computed from RRM on a hydrodynamic hypersurface at fixed longitudinal proper time of $\tau_f = 5.2(4.2)$ fm/c corresponding to the red (green) histogram.

increase by up to 30% for $p_T \simeq 5\text{-}7$ GeV.

Non-Prompt J/ψ .— The final component to be accounted for inclusive J/ψ measurements as performed by ALICE is the “non-prompt” contribution from weak-interaction decays of b -hadrons. We also utilize transported b -quark spectra with subsequent resonance recombination into B -mesons as computed in our transport model [30] (for simplicity, we do not resolve Λ_b baryons, although the total b -decay contribution is encoded in the fit to pp data). These are then decayed into J/ψ using the decay momentum distributions measured in Ref. [31]. The absolute differential yield of non-prompt J/ψ is determined in analogy to prompt feeddown contributions, based on the pp fit constructed in Fig. 1 left.

Inclusive J/ψ .— We obtain our final results for the inclusive $J/\psi R_{AA}$ in $\text{Pb-Pb}(5\text{ TeV})$ collision by adding the direct-suppressed and RRM components including their feeddown contributions as well as the non-prompt part from transported b quarks, in the numerator and divide by the denominator as described following Eq. (1). The elliptic flow, $v_2(p_T)$, is obtained by a weighted sum of the v_2 contributions of the individual components. The theoretical error bands represent the 15-25% shadowing effect on the p_T -dependent input distributions of primordial J/ψ and c -quarks. We find a rather good description of the ALICE data for both R_{AA} and v_2 , cf. Fig. 4, thus resolving the disagreement with previous transport model results. At intermediate p_T , the main effect is from the extended reach of the regeneration component due to the harder off-equilibrium charm-quark spectra, which significantly exceed previously employed blastwave spectra and thus figure with a larger weight than before, especially in the inclusive v_2 . It is also gratifying to see that the spatial dependence of the transported spectra, where the higher-momentum charm quarks tend to be more concentrated in the outer regions of the fireball,

play a non-negligible role. In addition, the considerable increase in the primordial v_2 at high p_T , from ~ 3 to $\sim 5\%$, is quite relevant for $p_T \gtrsim 5$ GeV. To illustrate the uncertainty of the regeneration temperature window, we also show results for a 20% reduced longitudinal proper time for the transport c -quark spectra ($\tau_f = 4.2\text{ fm}/c$), shown by the dashed lines in Fig. 4 (with a 15% integrated shadowing, to be compared to the upper edges of the bands for $\tau_f = 5.2\text{ fm}/c$). The R_{AA} is rather little affected by this change (mostly via a small enhancement at low p_T), but the v_2 is reduced by up to 15-20%. This is rather appreciable and may be used in future analysis to more precisely constrain the regeneration window. Since in our present treatment the regeneration temperatures represent *average* values, an explicit account of the time dependence of the c -quark phase space distributions, in connection with the underlying T -dependent dissociation rates and melting temperatures, will be in order.

Summary.— We have calculated the nuclear modification factor and elliptic flow of inclusive J/ψ production in heavy-ion collisions at the LHC. The main theoretical development was the implementation of state-of-the-art charm-quark phase distributions into the regeneration process of charmonia as obtained from a strongly coupled transport framework for heavy-flavor diffusion in QCD matter that describes open-charm observables at the LHC. Both the momentum and spatial dependences of these distributions (through off-equilibrium spectra and space-momentum correlations, respectively) were found to be instrumental in extending the relevance of recombination processes up to transverse momenta of about 8 GeV in semi-central $\text{Pb-Pb}(5\text{ TeV})$ collisions. In addition, an explicit calculation of the suppression of primordially produced charmonia leads to a significantly higher v_2 (caused by the path-length dependent dissociation) than previously estimated. We also utilized transported b -quark distributions to calculate the non-prompt portion of the inclusive J/ψ yields. Putting all these together, and without tuning any parameters, a good description of the experimental data for the R_{AA} and the v_2 of inclusive J/ψ 's emerged, thereby resolving discrepancies found in earlier transport model calculations. It is reassuring that this could be achieved through the quantitative coupling of the transport in the open- and hidden-charm sectors. In particular, our calculations exhibit significant sensitivity to the (average) production time of the J/ψ through its collectivity imprinted by the regeneration processes, where early production is disfavored by the magnitude of the v_2 and late production (with its larger radial flow) by the development of a characteristic “flow bump” in the R_{AA} that is not observed in the current data. In future precision analysis, aided by statistical tools, this could provide rather stringent constraints on the dissociation temperatures of the various charmonia. Our study can be straightforwardly extended into the bottom sector (where previous calculations for

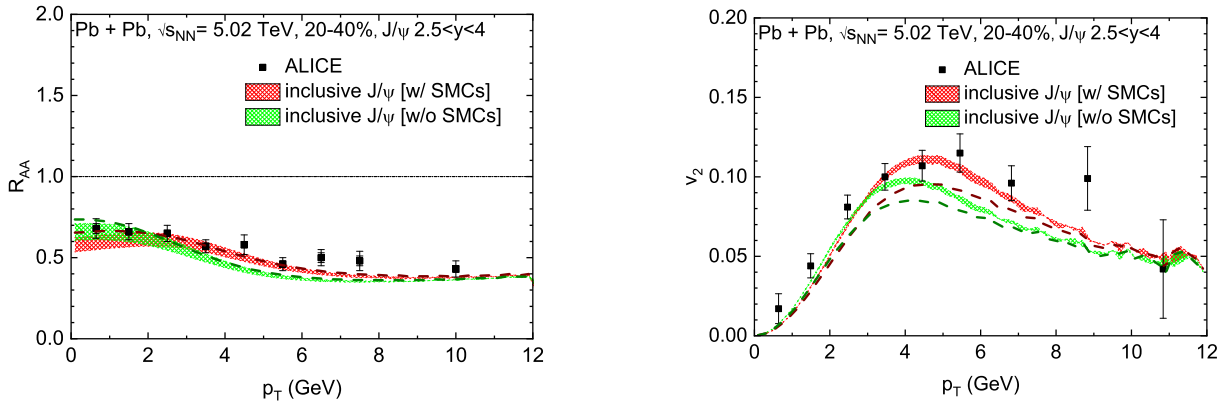


FIG. 4: Our results for the R_{AA} (left) and v_2 (right) of inclusive J/ψ production in 5 TeV Pb-Pb collisions at the LHC, compared to ALICE data [7, 14]. The red and green bands correspond to c -quark spectra figuring in RRM (with and without SMCs, respectively) evaluated at $\tau_f = 5.2 \text{ fm}/c$, where the band width reflects the 15–25% range of the integrated charm and charmonium shadowing. The dashed lines are the results for $\tau_f = 4.2 \text{ fm}/c$ for the case of 15% integrated shadowing only (brown-dashed: with SMCs, dark-green dashed: without SMCs).

Y production exist within a weak-coupling approximation [32, 33]), for B_c mesons, and for exotic quarkonia. While for Y mesons regeneration contributions are expected to be moderate [27], they are likely more important for the B_c and exotica [34], especially relative to their production in pp . Also for these observables our framework could contribute to a better understanding of the pertinent dissociation kinetics. Work in this direction is in progress.

Acknowledgments.— This work was supported by NSFC grant 12075122 and the U.S. NSF under grant no. PHY-1913286.

[1] R. Rapp, D. Blaschke and P. Crochet, *Prog. Part. Nucl. Phys.* **65**, 209 (2010).
[2] P. Braun-Munzinger and J. Stachel, *Landolt-Börnstein* **23**, 424 (2010).
[3] L. Kluberg and H. Satz, *Landolt-Börnstein* **23**, 372 (2010).
[4] A. Mocsy, P. Petreczky and M. Strickland, *Int. J. Mod. Phys. A* **28**, 1340012 (2013).
[5] A. Rothkopf, *Phys. Rept.* **858**, 1 (2020).
[6] J. Adam *et al.* [ALICE], *Phys. Lett. B* **766**, 212 (2017).
[7] S. Acharya *et al.* [ALICE], *JHEP* **02**, 041 (2020).
[8] S. Acharya *et al.* [ALICE], *Phys. Lett. B* **805**, 135434 (2020).
[9] X. Bai [ALICE], *Nucl. Phys. A* **1005**, 121769 (2021).
[10] A. Andronic, P. Braun-Munzinger, K. Redlich and J. Stachel, *Nucl. Phys. A* **789**, 334–356 (2007).
[11] L. Yan, P. Zhuang and N. Xu, *Phys. Rev. Lett.* **97**,

232301 (2006).
[12] X. Zhao and R. Rapp, *Nucl. Phys. A* **859**, 114 (2011).
[13] T. Song, K. C. Han and C. M. Ko, *Phys. Rev. C* **84**, 034907 (2011).
[14] S. Acharya *et al.* [ALICE], *JHEP* **10**, 141 (2020).
[15] K. Zhou, N. Xu, Z. Xu and P. Zhuang, *Phys. Rev. C* **89**, 054911 (2014).
[16] X. Du and R. Rapp, *Nucl. Phys. A* **943**, 147 (2015).
[17] S. Acharya *et al.* [ALICE], [arXiv:2110.09420 [nucl-ex]].
[18] [ALICE], ALICE-PUBLIC-2018-011.
[19] R. Aaij *et al.* [LHCb], *JHEP* **10**, 172 (2015) [erratum: *JHEP* **05**, 063 (2017)].
[20] S. Acharya *et al.* [ALICE], [arXiv:2108.02523 [nucl-ex]].
[21] R. Aaij *et al.* [LHCb], *Phys. Lett. B* **718**, 431–440 (2012).
[22] R. Aaij *et al.* [LHCb], *Eur. Phys. J. C* **72**, 2100 (2012) [erratum: *Eur. Phys. J. C* **80**, no.1, 49 (2020)].
[23] J. Adam *et al.* [ALICE], *JHEP* **06**, 055 (2015).
[24] M. He and R. Rapp, *Phys. Rev. Lett.* **124**, 042301 (2020).
[25] X. N. Wang and F. Yuan, *Phys. Lett. B* **540**, 62 (2002).
[26] X. Zhao and R. Rapp, [arXiv:0806.1239 [nucl-th]].
[27] X. Du, R. Rapp and M. He, *Phys. Rev. C* **96**, 054901 (2017).
[28] L. Ravagli and R. Rapp, *Phys. Lett. B* **655**, 126 (2007).
[29] M. He, R. J. Fries and R. Rapp, *Phys. Rev. C* **86**, 014903 (2012).
[30] M. He, R. J. Fries and R. Rapp, *Phys. Lett. B* **735**, 445–450 (2014).
[31] B. Aubert *et al.* [BaBar], *Phys. Rev. D* **67**, 032002 (2003).
[32] J. P. Blaizot and M. A. Escobedo, *JHEP* **06**, 034 (2018).
[33] X. Yao, W. Ke, Y. Xu, S. A. Bass and B. Müller, *JHEP* **01**, 046 (2021).
[34] B. Wu, X. Du, M. Sibila and R. Rapp, *Eur. Phys. J. A* **57**, no.4, 122 (2021).